August 27-31, 2023
FLORENCE - ITALY
16th International Conference on Wind Engineering
ICWE 16

Aerodynamic force prediction on the *DrivAer* car model by CFD: Impact of turbulence modeling approach

Peng Qin [1], Alessio Ricci [1,2], Bert Blocken [3]

[1]*Department of the Built Environment, Building Physics and Services, Eindhoven University of Technology, Eindhoven, The Netherlands, p.qin@tue.nl - a.ricci@tue.nl - b.j.e.blocken@tue.nl*
[2]*Department of Science, Technology and Society, University School for Advanced Studies IUSS Pavia, Piazza della Vittoria 15, 27100, Pavia, Italy, alessio.ricci@iusspavia.it*
[3]*Department of Civil Engineering, Building Physics and Sustainable Design, KU Leuven, Leuven, Belgium, bert.blocken@kuleuven.be*

SUMMARY:
Automotive designers and engineers are constantly working on the optimization of aerodynamic performance of vehicles to reduce fuel consumption and gas/particulate emissions. In recent decades, among several car models, the *DrivAer* model has become one of the most adopted car bodies in general studies of automotive aerodynamics. Although wind-tunnel (WT) testing and Computational Fluid Dynamics (CFD) are systematically used to investigate the aerodynamic performance of cars, it is still unclear to what extent CFD results might be affected by computational parameters as the turbulence modeling approach. This is also the goal of the present paper for which the impact of RANS, SAS, SBES and LES approaches on the prediction of the aerodynamic performance (i.e. drag and lift coefficients) of a scaled 1:4 *DrivAer* model is investigated. The CFD results were validated with the WT data. The comparison showed that SAS, SBES and LES generally outperform the 3D steady RANS approach especially for the C_L prediction.

Keywords: DrivAer model, CFD simulations, aerodynamic forces.

1. INTRODUCTION
Cars, trucks, and motorbikes as main transportation items are responsible for more than 40% of nitrogen oxides (NOx) emissions and particulate matter in the European Union (EEA, 2020). Automobile designers and engineers are constantly engaged in an effort to optimize vehicle body shapes with the aim of reducing the aerodynamic drag, fuel consumptions and particle emissions. Wind-tunnel (WT) testing of full and reduced-scale models and Computational Fluid Dynamics (CFD) are commonly used to investigate the aerodynamic performance of such vehicles worldwide (Ekman et al., 2019). Real and simplified models are usually used for WT tests and CFD simulations. However, to bridge the gap between these two categories the *DrivAer* model (Heft et al., 2012), a mix of Audi A4 and BMW 3 Series, has been developed. This car model has rapidly become one of the most adopted car bodies for experimental and numerical investigations. Despite many efforts towards the definition of a numerical benchmark of the *DrivAer* model, it is still unclear to what extent the CFD results may be affected by some computational parameters, as the turbulence modeling approach. This is also the goal of the present study which aims at investigating the impact of 3D steady Reynolds-Averaged Navier-Stokes (RANS), scale-adaptive simulation (SAS), stress-blended eddy simulation (SBES) and

large eddy simulation (LES) on the prediction of the aerodynamic forces on the *DrivAer* model with a notchback geometry. The CFD results are analyzed in terms of drag and lift coefficients (C_D and C_L) and compared to the corresponding WT data.
The paper is organized as follows: Section 2 describes the WT setup; Section 3 describes the computational settings; Section 4 discusses the impact of turbulence modeling approaches (i.e. RANS, SAS, SBES and LES) on the aerodynamic forces; Section 5 closes the paper with conclusions and perspectives.

2. WIND-TUNNEL TESTING

WT tests were performed at the closed-loop atmospheric boundary layer wind tunnel (ABLWT) of the Eindhoven University of Technology (TU/e, in the Netherlands). The WT facility has a test section of 3 m (width) × 2 m (height) × 27 m (length). A scale of 1:4 was chosen for the *DrivAer* model. Figure 1 shows the side and front views of the car model mounted on the platform. Four 3-component sensors of K3D type with an accuracy of 0.5% for each component were used to measure the aerodynamic forces (F_D and F_L). F_D and F_L are the horizontal and vertical forces in *x*-direction and *z*-direction, respectively (Fig. 1a,b). Each sensor was connected to the model's wheel by means of a stiff pin in order to avoid any possible displacement of the car during the tests. The aerodynamic forces were quantified in terms of drag (C_D) and lift (C_L) coefficients by Equation 1:

$$C_{(D,L)} = \frac{F_{(D,L)}}{0.5\rho U_{ref}^2 A} \tag{1}$$

where ρ is the density of air (kg/m³), U_{ref} indicates the reference wind speed (m/s) measured at an undisturbed position taken upstream of the model, and A is the frontal area (m²) of the *DrivAer* scaled (1:4) model.

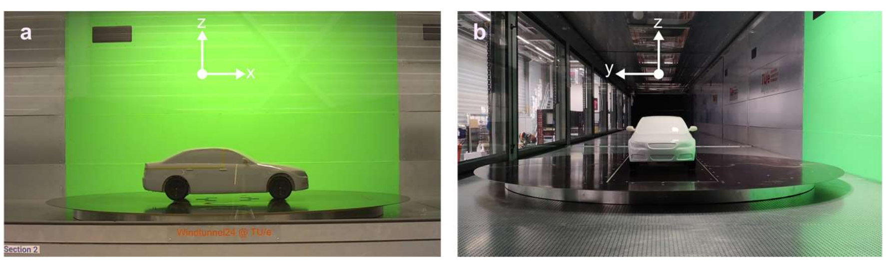

Figure 1. Photos of the scaled *DrivAer* model (1:4) mounted on the sharped-edged plate in the ABLWT of TU/e.

3. CFD SIMULATIONS: COMPUTATIONAL SETTINGS AND PARAMETERS

3.1. Computational geometry, domain and grid

The CFD simulations were performed on the same reduced-scale model described in Section 2 and Figure 1. The computational geometry of the car was obtained by scanning the model previously tested to ensure the conformity between WT and CFD, and for the same reason the domain was generated by reproducing a portion of the ABLWT test section. Therefore, the width and height of the domain were the same as the WT cross-section and the sharp-edged platform supporting the car (Fig. 1b) was also reproduced. The upstream and downstream distances from the car model to the inlet and outlet faces were set equal to 3 and 7 times the length (L) *DrivAer* car model, respectively. The grid was constructed by referring to previous CFD studies conducted on the *DrivAer* model (e.g. Zore et al., 2019). The software ANSYS Fluent (Ansys, 2018) was used for the construction and simulation of the computational grid. A grid-sensitivity analysis (GsA) was performed with three grids having a different level of refinement: *coarse* (about 10 million cells), *medium* (about 31 million cells), and *fine* (about 42 million cells). Based on the GsA results, the *medium* grid was adopted for further analysis.

3.2. Boundary conditions and other settings

A uniform wind speed (U_{ref} = 30 m/s) and a constant turbulence intensity (I_{ref} = 1%) were imposed on the inlet face to accurately reproduce the WT flow conditions. The spectral synthesizer method was used as turbulence inflow generator for SAS, SBES and LES simulations. At the outlet face zero-static gauge pressure was imposed. The no-slip wall condition was imposed at the top (i.e. WT ceiling), side (i.e. WT lateral walls) and bottom (i.e. WT ground) of the domain in order to reproduce the boundary layer on the WT walls. Four turbulence modeling approaches were tested: the 3D steady RANS coupled with shear-stress transport (SST) k-ω turbulence model, the SAS coupled with SST k-ω, the SBES coupled with SST k-ω and the LES. The least square cell-based scheme was used for the gradient calculation, the second-order interpolation was used for the pressure and the bounded central differencing scheme was used for the momentum. For RANS, the coupled algorithm was adopted for pressure-velocity coupling and the pseudo-transient method with a time step size of 0.01 s was adopted to facilitate the numerical convergence. A total of 6000 iterations were run and the final solution was obtained by averaging the last 4000 iterations. For SAS, SBES and LES, the PISO algorithm was used for pressure-velocity coupling. The time-step size was set equal to 1.0e-5 s for SAS and SBES, and equal to 5.0e-7 s for the LES in order to keep the maximum Courant-Friedrichs-Lewy (CFL) number below 20 and 1, respectively. For each time step a fixed number of 10 inner iterations was equally defined for the three time-dependent approaches. The SAS, SBES and LES simulations were initialized with the final RANS solution, such as a total of 30 convective flow units (i.e. 30 CFUs = 30 L/U_{ref}). The first 10 CFUs were used to erase the initial effect of 3D steady RANS, while the other 20 CFUs were used for the time-averaging of the solution.

4. IMPACT OF TURBULENCE MODELING APPROACH

Figure 2 shows the comparison of C_D and C_L for the selected turbulence modeling approaches and the relative difference (%) with respect to the WT results. In general, the SAS, SBES and LES results show a better agreement to WT data with respect to RANS. For the C_D, deviations of about ±1.0% and +5.5% are found with respect to WT data for the SAS/SBES/LES and RANS, respectively. For the C_L, a less satisfactory agreement is found between RANS and WT with a deviation of +26.3%. On the contrary, a better agreement is observed for the SAS (+4.6%, overestimation of WT data), the SBES (-7.7%, underestimation of WT data) and the LES (-2.3%, underestimation of WT data).

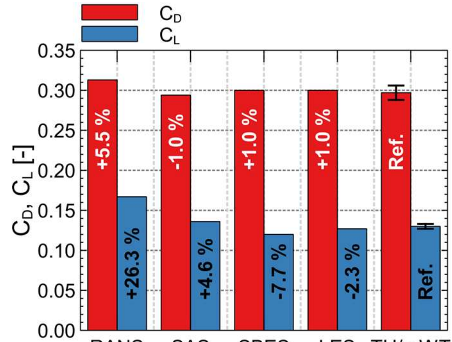

Figure 2. Impact of turbulence modeling approaches on C_D and C_L. WT results are also reported for comparison.

To deeply understand the aforementioned deviations and the dynamics of the flow around the car, the *Q-criterion* (colored by $|V|/U_{ref}$) was used to visualize the coherent turbulent structures ($Q = 3\times10^5\ s^{-2}$), by means of iso-surface plotted for RANS (Fig. 3a) and SAS/SBES/LES (Fig. 3b). Some general observations are made:

- Instantaneous coherent turbulent structures cannot be provided for RANS since this is a no-time dependent approach.
- From the center of the roof up to the wake region, the SAS/SBES/LES approaches show a slightly different performance, with LES providing better resolved small-scale turbulent structures.
- At the upper edge of the rear windshield, a separation region of the flow is observed with small-scale vortical structures increasing in size towards the wake region for SAS/SBE/LES (more visible with LES).
- At the tail, larger separations are predicted by SAS/SBES/LES (more visible with LES) leading to vortical structures increasing in size from the core (region of lower wind speed) to the outer parts (region of higher wind speed).

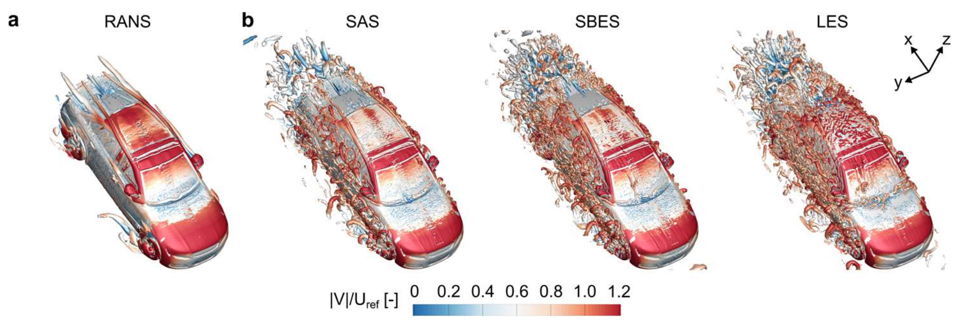

Figure 3. Coherent turbulent structures around the car in terms of iso-surface visualized with the *Q-criterion* (colored by $|V|/U_{ref}$) for the four analyzed cases: (a) RANS, (b) SAS, (c) SBES and (d) LES.

5. CONCLUSIONS AND PERSPECTIVES

Hybrid RANS-LES (i.e. SAS and SBES) and transient (i.e. LES) approaches provided a good agreement in terms of C_D and C_L with WT data. These three approaches generally outperform the 3D steady RANS especially as far as the C_L prediction is concerned. These results are better elucidated by the Q-criterion plots, where the SAS, SBES and LES yield slightly different instantaneous fields, with the LES better resolving small-scale vortical structures than SAS and SBES. Additional results will be discussed in more detail in the full paper.

REFERENCES

Ansys Inc., 2018. ANSYS Fluent Theory Guide 19.2.

EEA, 2020. SIGNALS 2020 - Towards zero pollution in Europe.

Ekman, P., Larsson, T., Virdung, T. and Karlsson M., 2019. Accuracy and speed for scale-resolving simulations of the DrivAer reference model. SAE Technical Papers.

Heft, A.I., Indinger, T. and Adams, N.A., 2012. Introduction of a new realistic generic car model for aerodynamic investigations. SAE Technical. Papers.

Zore, K., Caridi, D., Lockley, I., 2019. Fast and Accurate Prediction of Vehicle Aerodynamics Using ANSYS Mosaic Mesh. SAE Technical Papers.